N86-17844

N/P GaAs CONCENTRATOR SOLAR CELLS WITH AN IMPROVED GRID AND BUSBAR CONTACT DESIGN

Gregory C. DeSalvo, Ervin H. Mueller, and Allen M. Barnett*
University of Delaware
Newark, Delaware

1. GaAs Solar Cell

The major requirements for a solar cell used in space applications are high efficiency at AMO irradiance and resistance to high energy radiation. Gallium arsenide, with a band gap of 1.43 eV, is one of the most efficient sunlight to electricity converters (25%) when the simple diode model is used to calculate efficiencies at AMO irradiance. GaAs solar cells are more radiation resistant than silicon solar cells and the N/P GaAs device has been reported to be more radiation resistant than similar P/N solar cells [1]. This higher resistance is probably due to the fact that only 37% of the current is generated in the top N layer of the N/P cell compared to 69% in the top layer of a P/N solar cell. This top layer of the cell is most affected by radiation. It has also been theoretically calculated that the optimized N/P device will prove to have a higher efficiency than a similar P/N device [2].

This N/P GaAs solar cell will have a thin GaP window layer to reduce the minority carrier surface recombination velocity from 10^6 cm/sec to 10^4 cm/sec. GaP has been chosen as the window layer material instead of $Ga_xAl_{1-x}As$ to insure the formation of ohmic contacts that do not suffer degradation upon exposure to air. The problem of the 3.6% lattice mismatch between GaAs and GaP will be minimized by keeping the thickness of the epitaxially grown window layer thin enough so that its lattice constant may be strained elastically to equal that of the underlying GaAs.

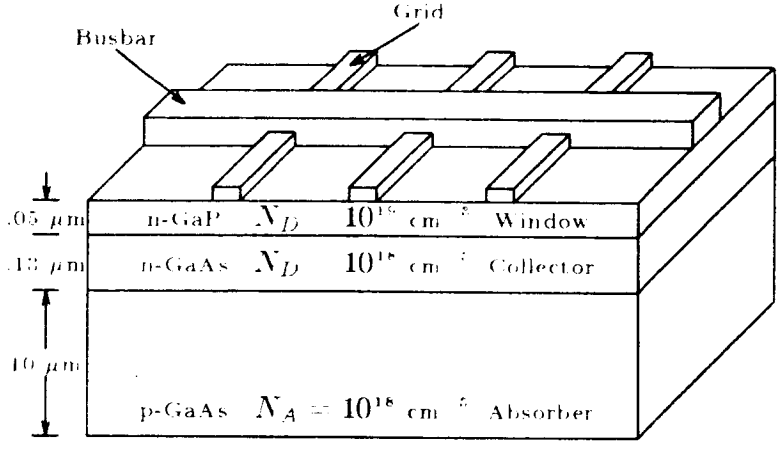

Figure 1 Optimized N/P GaAs solar cell

This work supported by the NASA Lewis Research Center under contract NAG3-422.

The optimized N/P GaAs solar cell with a thin GaP window layer is shown below in Figure 1 along with theoretical efficiencies and a loss analysis [2].

Table 1

Calculated Theoretical Efficiencies and Loss Analysis for N/P GaAs

Loss Mechanism	% Loss	J_{sc} mA/cm^2	V_{oc} volts	Fill Factor	AM0 η 1 Sun
Theoretical Maximum	—	38.6	1.09	.892	27.7
Recombination	4.7	36.8	1.07	.891	25.9
a. Top Layer	1.6	13.6*	—	—	—
b. Bottom Layer	3.1	18.8*	—	—	—
Absorption	1.0	36.4	1.07	.890	25.6
Reflection	2.6	35.4	1.07	.890	24.9
Grid Transparency	4.0	34.0	1.07	—	—
Resistive	4.6	—	—	.890	23.9

* The balance of J_{sc} is generated in the depletion region
$\therefore\ J_{sc} = J_{top} + J_{bottom} + J_{depl}$

2. Top Contacts

The generic solar cell structure, including grid lines and busbars, is shown in Figure 2. The top contacts are designed to remove the generated current from the solar cell. Ideally, grid lines act as the primary current collectors and receive all of the current from the semiconductor region. Busbars are the secondary collectors which pick up current from the grids and carry it out of the active region of the solar cell. This separation of functions allows for a multi-layer metallization design, so that busbars can be made larger (in cross section) than the grids since they carry more current. This multi-layer design is usually not used, even when grid optimization is performed [3–5], however, this design can be shown to provide a higher efficiency solar cell [6].

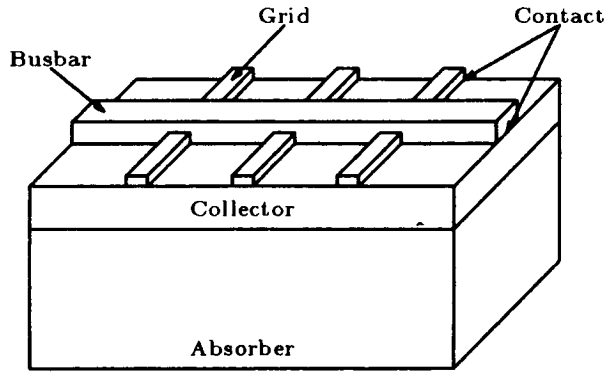

Figure 2 Generic solar cell.

2.1 Grid Losses

The grid pattern contains several loss mechanisms which reduce the available output power. Unlike many losses which are dependent on basic physical principles or intrinsic material properties, the grid losses are mainly dependent on engineering design. Thus, by using loss minimization [7], an optimum grid geometry can be found which provides for the best output power for a given solar cell.

Top contact losses consist mainly of electrical (I^2R) losses and optical losses (transparency/shading). A mathematical description of these grid losses is necessary in order to perform loss minimization.

Electrical Losses — These losses are basically due to ohmic losses (heating) incurred during removal of power from the solar cell. The geometry of the grid affects the current flow throughout the cell, so each region will have a loss component [Figure 2]. The total electric power loss can be modelled as the sum of these individual loss components [7].

$$P_{loss} = I^2 R_{loss} = I^2(R_{absorber} + R_{collector} + R_{grid} + R_{busbar}) \tag{1.1}$$

Optical Losses — The top contacts block some of the light that would normally enter the solar cell. This optical loss can be defined in terms of the percentage of light that penetrates to the active region of the solar cell (i.e., the transparency T).

$$T \overset{\text{def}}{=} \frac{SA_{cell} - SA_{grids/busbars}}{SA_{cell}} \qquad (0 \leq T \leq 1) \tag{1.2}$$

where SA is the surface area.

The minimizing process requires a low electrical loss (R_{loss} small) as well as a low optical loss ($T \rightarrow 1$). Since both processes compete with each other, a compromise must be reached to obtain the minimum total grid loss. By describing the photogenerated current in terms of a percentage (T) of the maximum possible current I_{max}, both losses can be combined into a single "power loss equation."

$$I_{light} = qA\eta\phi = qA\eta(\phi_{max}T) = I_{max}T \tag{1.3}$$

$$P_{loss} = (I_{max}T)^2(R_{abs} + R_{coll} + R_{grid} + R_{bus}) \tag{1.4}$$

Finally, using Poynting's vector, a description of the current flow in point form can be derived for P_{loss}, such that:

$$P = \int_V J^2 \rho \, dV \equiv (I_{max}T)^2 R_{loss} \tag{1.5}$$

In this form, the current density $\vec{J}(x, y, z)$ can be described thoroughly in any region of the solar cell. Solution of the integral for each solar cell region can then be compared to $(I_{max}T)^2 R_{region}$ to determine the "lumped resistance" belonging to that region. Once each R_{region} has been found, the total top contact resistance R_{loss} can be minimized.

2.2 Current Flow in a Solar Cell

A schematic of how current might flow in an actual cell is given by Figure 3a.

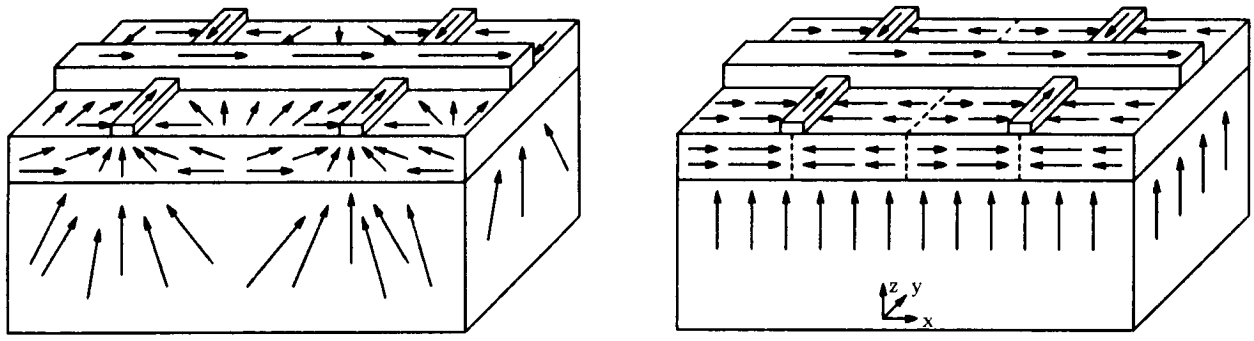

Figure 3 (a) Actual current flow model in a solar cell and (b) theoretical current flow.

This description can be simplified without significant error by using several useful assumptions:

1. Solar cell operates at the short circuit current point.
2. Uniform photon flux ϕ is incident over the entire x y planar surface of the cell.
3. Uniform current generation rate throughout the cell.
4. Constant current density enters the collector region from the absorber region in the z direction.
5. Thickness of collector region (t) is much smaller than lateral x y dimensions.
6. Grid/Busbar contacts are equipotentials

$$\rho_{grid}, \rho_{busbar} \ll \rho_{absorber}, \rho_{collector}$$

7. Resisitivities are uniform within a given region.

$$\rho_{region}(x, y, z) \equiv \rho_0$$

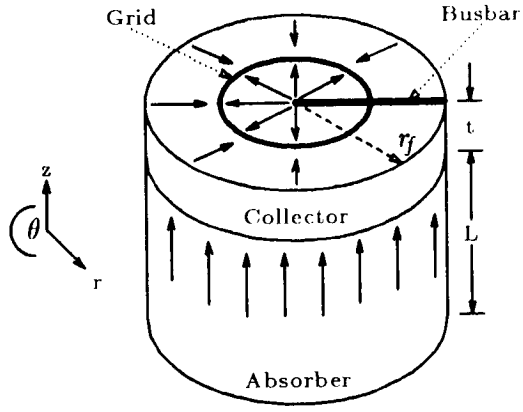

Figure 4 Cylindrical solar cell model.

The resulting theoretical current flow is shown in Figure 3b. However, an optimum grid pattern for a solar cell concentrator is desired. Since the spot of illumination will be circular in nature, a circular grid design is suggested. Figure 4 shows a cylindrical solar cell model with a theoretical current flow using these same assumptions.

2.3 Solution of R_{loss}

The easiest means of solving R_{loss} is to individually solve for each R_{region}. The general placement of the grids and busbars is shown in Figure 4. The grids are circular rings and the busbars project radially from the center of the solar cell. For a circular solar cell, current traveling to a grid will be parabolic ($J(r) \propto r^2$) since the area increase as r^2. If grids are placed to inscribe equal areas, then each grid will receive an equal amount of the total current.

$$\text{Grid placement} \qquad R_l = \sqrt{\frac{2l-1}{2N}}\, r_f \qquad l = 1, 2, 3, \ldots, N \text{ Grids} \tag{1.6}$$

Radial busbars provide the shortest path out of the solar cell while intersecting each grid once. Tapered busbars are used for ease of calculation in cylindrical coordinates. Once the current densities in each region have been determined, the power loss equation (2.4) can be solved, yielding the individual resistances.

$$R_{abs} = \frac{\rho_{abs} L}{\pi r_f^2} \tag{1.7}$$

$$R_{coll} = \frac{\rho_{coll}\, \pi r_f^2}{32\pi l N^2} \sum_{l=1}^{N} \left[8l^2 \ln \frac{2l}{2l-1} + 2(2l-2)^2 \ln \frac{2l-1}{2l-2} - 8l + 4 \right] \tag{1.8}$$

$$R_{grid} = \frac{\rho_{grid}\, \pi r_f}{6NM^2 w_g t_g} \sum_{l=1}^{N} \sqrt{\frac{2l-1}{2N}} \tag{1.9}$$

$$R_{bus} = \frac{\rho_{bus}\, r_f}{4M w_b t_b} \tag{1.10}$$

$$T = \frac{\pi r_f^2 - \left[2\pi r_f w_g \sum_{l=1}^{N} \sqrt{\frac{2l-1}{2N}} - \frac{1}{2} M w_b r_f \right]}{\pi r_f^2} \tag{1.11}$$

Grids are made at the narrowest practical limit (with $\frac{t_g}{w_g} = 2$), and this ratio is maintained as dimensions are increased ($\frac{t_b}{w_b} = 2$). So, a scale factor (m) can be introduced to represent the larger busbar dimensions (w_b, t_b) relative to the grid line dimensions (w_g, t_g). That is:

$$\left.\begin{aligned} t_b &= m t_g \\ w_g &= m w_g \end{aligned}\right\} \qquad \frac{t_b}{w_b} = \frac{m t_g}{m w_g} = 2 \tag{1.12}$$

2.4 Grid Optimization

The optimum grid pattern can be found by solving the output power equation (2.4). The criterion for the best grid pattern occurs when the output power (P_{out}) is at a maximum (i.e., when P_{loss} is minimized).

$$P_{out} = P_{max} - P_{loss} \tag{1.13}$$

$$P_{max} = I_{max} V_{max} T \tag{1.14}$$

$$P_{loss} = (I_{max} T)^2 R_{loss} \tag{1.15}$$

A computer program was written to calculate and find the maximum output obtainable by varying the three unknowns (N, M, and m), and using the given design parameters (Table 2) for the GaAs solar cell concentrator. An example of one optimized grid pattern for 1000 · AM0 sunlight is shown in Figure 5, with numerical results given in Table 3.

Table 2

N P GaAs Input Parameters for Grid Optimization					
$J_{sc}^{1\times}$	35.4 $\frac{mA}{cm^2}$	L	10 μm	ρ_{abs}	1.56×10^{-2} Ω cm
$V_{oc}^{1\times}$	1.07 V	t	.13 μm	ρ_{coll}	7.10×10^{-5} Ω cm
$\times$	1000	w_g	10 μm	ρ_{grid}	1.68×10^{-6} Ω cm
r_f	2 mm	l_g	5 μm	ρ_{bus}	1.68×10^{-6} Ω cm

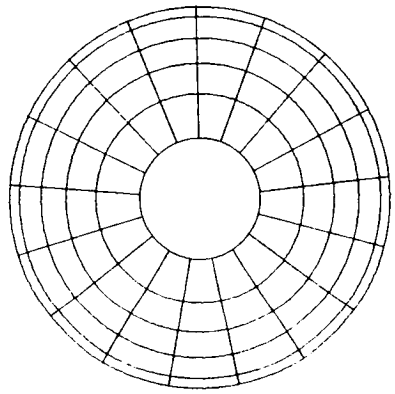

Figure 5 Optimized grid pattern for 1000$\times$ AM0.

Table 3

Numerical Results from the Best Grid Pattern		
$J_{sc}^{1000\times}$ = 35400 $\frac{mA}{cm^2}$	η = .9172	R_{abs} = .1243 mΩ
$V_{oc}^{1000\times}$ = 1.249 V	T = .9479	R_{coll} = 5.656 mΩ
I_{max} = 4.351 mA	N = 5	R_{grid} = .8167 mΩ
V_{max} = 1.150 V	M = 17	R_{bus} = 2.444 mΩ
P_{max} = 5.003 W	m = 2	R_{loss} = 9.041 mΩ

2.5 Multi-Layer Metallization

A comparison between single layer and multi-layer grids is given in Table 4. The multi-layer design has its maximum impact at higher concentrations and larger cell areas (i.e., high currents). A pictorial comparison of the transparency savings with a multi-layer grid pattern is shown in Figure 6.

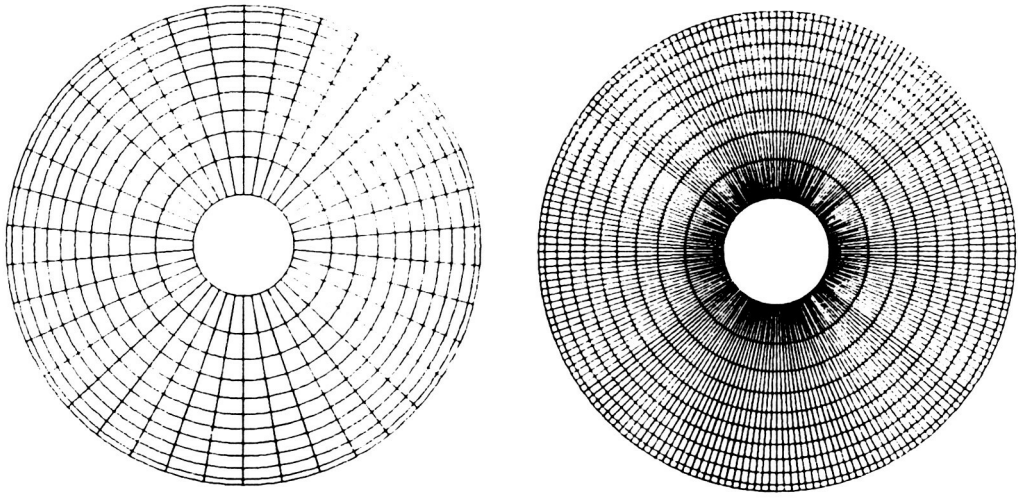

Figure 6 Comparison of thick busbar vs. thin busbar pattern: (a) 11 grids, 38 busbars, 4 scale (m) (b) 10 grids, 200 busbars, 1 scale (m).

Table 4

Diameter (cm)	Concentration ($\times$)	Thick Busbar (η)	Thin Busbar (η)	Improvement (%)
1.0	100	.9447	.9293	1.66
	300	.9129	.8832	3.36
	1000	.8605	.8016	7.35
2.0	100	.9160	.8728	4.95
	300	.8703	.7931	9.73
	1000	.7944	.6606	20.25

2.6 Experimental Results

The computer program provides specific power losses for each of the semiconductor and metal layers as part of the optimization. These theoretical values were compared to another grid program from Sandia National Laboratories [8, 5] and found to give similar results for the same grid design.

Several experimental test solar cells were made using the grid pattern described in Figure 5. The solar cell is N/P GaAs and closely matches the optimum design given in Figure 1 (but

with a GaAlAs window). A picture of a test cell is shown in Figure 7 along with an I V curve measured on a curve tracer.

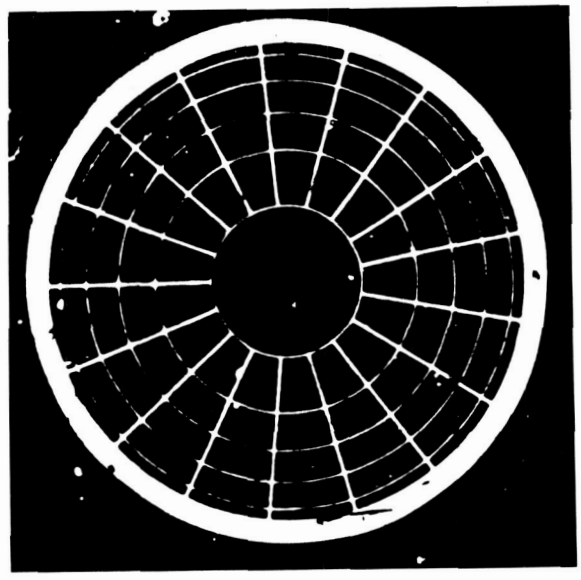

Figure 7 Experimental solar cell with optimized grid pattern.

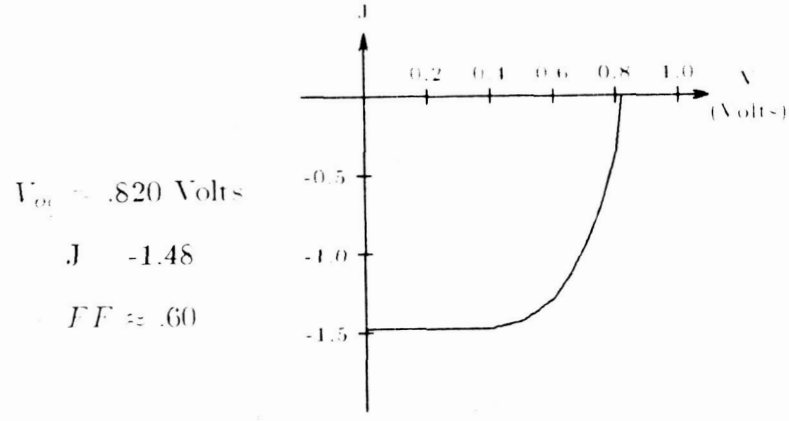

Figure 8 I V curve of experimental solar cell.

3. Conclusions

The use of a GaP window layer on a GaAs solar cell will avoid many of the inherent problems normally associated with a GaAlAs window, while still proving good passivation of the GaAs surface. An optimized circular grid design for solar cell concentrators has been shown which incorporates a multi-layer metallization scheme. This multi-layer design allows for a greater current carrying capacity for a unit area of shading, which results in a better output efficiency.

References

1 C. Amano, M. Yamaguchi, and A. Shibukawa, "Optimization of Radiation-Resistant GaAs Solar Cell Structures," Tech. Digest International PVSEC-1, Kobe, Japan (1984), p. 11.

2 R.H. Parekh and A.M. Barnett, "Improved Performance Design of GaAs Solar Cells for Space," IEEE Trans. Electron Devices, **ED-31**, 689 (1984).

3 M. Wolf, "Limitations and Possibilities for Improvement of Photovoltaic Solar Energy Converters," Proceedings of the IRE, **48**, 1246 (1960).

4 R.S. Sharlack, "The Optimal Design of Solar Cell Grid Lines," Solar Energy, **23**, 199 (1979).

5 P.A. Basore, "Optimum Grid-Line Patterns for Concentrator Solar Cells under Nonuniform Illumination," IEEE 17th Photovoltaics Specialists Conference, Kissimmee, FL (1984), p. 637.

6 A. Flat and A.G. Milnes, "Optimization of Multi-Layer Front-Contact Grid Patterns for Solar Cells," Solar Energy, **23**, 289 (1979).

7 A.M. Barnett, "Analysis of Photovoltaic Solar Cell Options," 16th IEEE Photovoltaics Specialists Conference, San Diego, CA (1982), p. 1165.

8 Program courtesy of J.M. Gee, Sandia National Laboratory. Program written by P.A. Basore.